

## First Steps towards the Development of a New Bio-optoelectronic Device with a Functioning Protein on a Silicon Substrate

*Koji Sumitomo<sup>†</sup>, Hiroshi Nakashima, Mime Kobayashi, Keiichi Torimitsu, Chandra Ramanujan, and John F. Ryan*

### Abstract

The combination of biological systems with artificially fabricated nanoscale structures offers the potential for developing new electronic, photonic, and biosensing molecular-scale devices. In this study, we investigated the use of bacteriorhodopsin (bR), the photoreceptor protein in purple membrane, to form the basis of new optoelectronic devices using nanofabricated silicon structures. The periodical hexagonal shape of bR was observed in liquid by atomic force microscopy. Imaging the suspended purple membrane over artificially fabricated cells is an essential first step in developing a device with a functioning protein. We found that slight modification of the silicon surface or difference in the salt concentration of the buffer affected how the bR attached to the surface. We are still at a very early stage on the road toward optoelectronic devices on a silicon surface.

### 1. Introduction

Molecular and biomolecular electronics have been studied extensively in the last decade because they promise better performance at a lower production cost than conventional silicon-based integrated circuits [1]. The combination of biological systems and semiconductor nanotechnology has great potential for device applications [2].

Initially, at least, we are investigating the photoreceptor bacteriorhodopsin (bR) because it has well-characterized optical and electrical properties. It is a robust protein found in the purple membrane of the salt-loving microorganism *Halobacterium salinarum*, which was discovered more than three decades ago in the extreme environment of salt marshes [3]. It is typical of the class of photochromic proteins, and it functions as a light-driven proton pump and enables the organism to survive at extremely high salt concentrations using sunlight as the sole

source of energy (**Fig. 1**) [4]. Two important properties have driven enormous interest in device applications of bR. First, it serves as a simple model for cell-membrane photoreceptors: the photosensitivity and ability to switch functions in response to illumination of this biological photochromophore are far superior to those of synthetic materials. Second, it serves as a prototype of a membrane transporter: it transports ions against an electrochemical potential [5]. Unveiling the mechanisms behind the physical functions of bR is an appealing way to learn from biological molecules in order to develop new electronic devices.

A lot of studies have been conducted to analyze and understand its structure and biological functions [3]-[17]. Purple membrane consists of two-dimensional (2D) crystals of 75% bR protein and 25% lipid derivatives [6], [7]. Trimers of bR are regularly arranged in the purple membrane to form a hexagonal lattice (**Fig. 2**). The bR protein consists of seven transmembrane alpha-helical<sup>\*1</sup> structures (A to G), linked by

<sup>†</sup> NTT Basic Research Laboratories  
Atsugi-shi, 243-0198 Japan  
E-mail: sumitomo@will.brl.ntt.co.jp

\*1 Alpha helix: A common structure found in proteins, characterized by a single, spiral chain of amino acids (polypeptide) stabilized by hydrogen bonding.

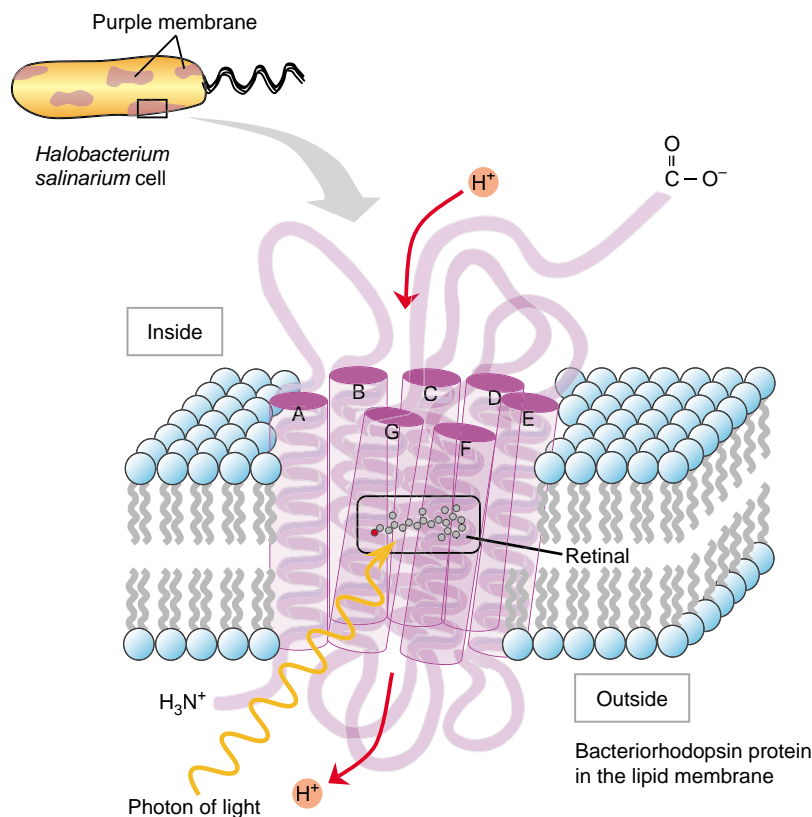


Fig. 1. Schematic illustration of bacteriorhodopsin (bR) protein in purple membrane.

short loops on either side of the membrane [8], [9]. The chromophore<sup>\*2</sup> retinal is connected via a Schiff base<sup>\*3</sup> to the nitrogen atom of a lysine<sup>\*4</sup> –216 residue in helix G [10]. Upon absorption of light in the visible spectral region, retinal changes its configuration from the all-*trans* form to the 13-*cis* form, which takes about one picosecond. The photoisomerization<sup>\*5</sup> triggers the transport of a proton from the cytoplasmic to the extracellular side, and an electrochemical potential of up to 250 mV is thus generated across the membrane. This potential translates into a 10,000-fold difference in proton concentration. The resulting proton gradient is used to synthesize ATP<sup>\*6</sup>, which is the universal energy source of living organisms. The bR undergoes structural changes during the unidirectional proton pumping: a series of intermediates, referred to as K, L, M, N, and O states that have different colors, have been well characterized by optical absorption spectroscopy [11]. Since the mid-1980s, the photoinduced electrical effects arising from the proton transport have been studied in an artificial cell using metal electrodes and electrolytic medium [12]. Sensory aspects of the bR molecule have also been demonstrated in a completely solid

device [11], [13].

In this paper we describe a model device with biomolecular function obtained from electrically contacted artificially fabricated cells, as shown in **Fig. 3**. The device consists of a purple membrane (bR protein and lipid) covering a small cell (submicrometer dimensions) fabricated on a Si substrate and electrodes attached to them. These cells can contain proteins that are chosen or modified according to the

\*2 Chromophore: The part of a molecule responsible for its color. In biological molecules that serve to capture or detect light energy, the chromophore is the moiety that causes a conformational change of the molecule when exposed to light.

\*3 Schiff base: A base structure containing  $R^1N=CHR^2$  or  $R^1N=CR^3R^4$  chemical bonds, which are obtained by the reaction between primary amine ( $R^1N-H_2$ ) and aldehyde ( $R^2CHO$ ) or ketone ( $R^3COR^4$ ).

\*4 Lysine: One of the essential amino acids. Lysin-216 indicates the 216th amino acid from the  $NH_3^+$ -end of successively connected amino acids (polypeptide).

\*5 Photoisomerization: Structural change of a molecule between isomers (e.g., retinal: from the all-*trans* to the 13-*cis* form) caused by photoexcitation.

\*6 ATP: Adenosine triphosphate (ATP) is synthesized from adenosine diphosphate (ADP) and inorganic phosphate using the electrochemical potential of protons.

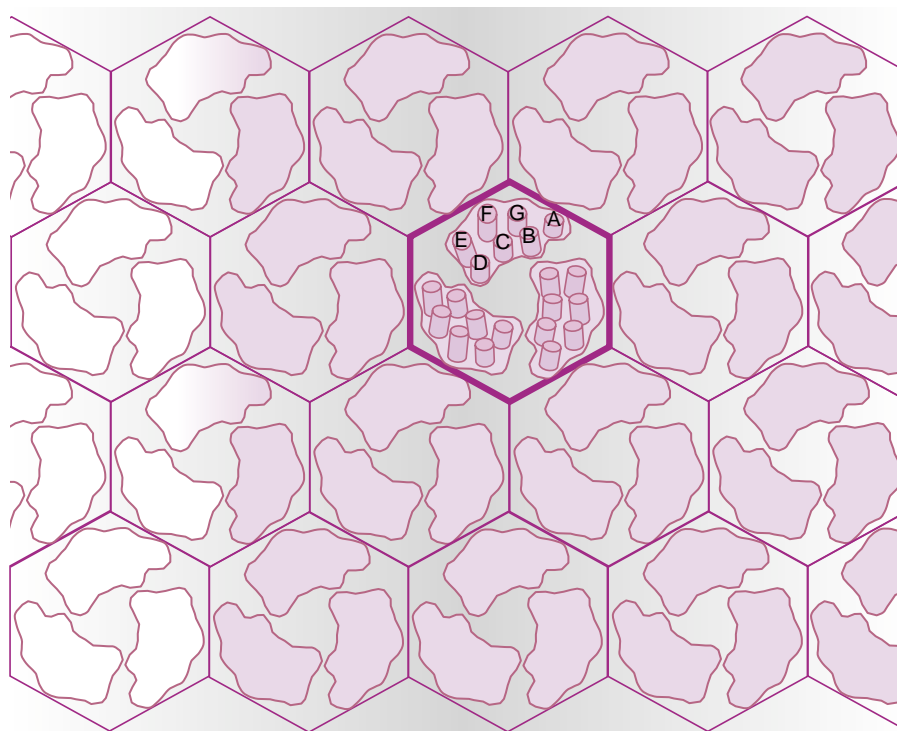


Fig. 2. Schematic illustration of 2D crystal of bR in purple membrane (cytoplasmic side).

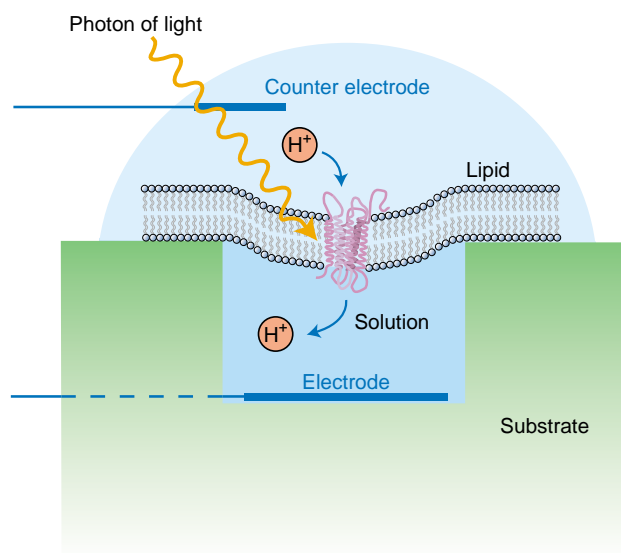


Fig. 3. Schematic drawing of a purple membrane-Si optoelectronic device.

functional needs of the device. For example, if a photoactive membrane protein such as bR is used to cover cells, the flow of ions through the membrane could be controlled by photons of light. The cell must be filled with electrochemical buffer solution such as KCl. Photons of light control the gating of the ion

channel in a purple membrane and it is expected to act as a transistor by utilizing the gating function of the membrane protein. The integration of a number of different proteins on such a multi-cell substrate could provide novel functionality.

## 2. Results and discussion

### 2.1 AFM images of purple membranes on mica

In order to utilize membrane proteins like bR in the fabrication of nanoscale devices, as shown in Fig. 3, functional or structural changes of the protein should be monitored at the nanoscale, i.e., on the molecular scale, and under physiological conditions, i.e., in liquid. To confirm the exact location of membrane protein on the optoelectronic device, we decided to use a commercial atomic force microscope (AFM: Dimension 3100, Veeco Instruments Inc., USA). Although electron microscopy, nuclear magnetic resonance (NMR), and X-ray diffraction techniques with high spatial resolution have been used with great success for structural analysis of biological molecules, these techniques require samples to be in a static condition (low temperature) or in vacuum. On the other hand, AFM has been widely used for imaging biological molecules in liquid with nanometer resolution [18]. In AFM measurements, the very weak atomic force

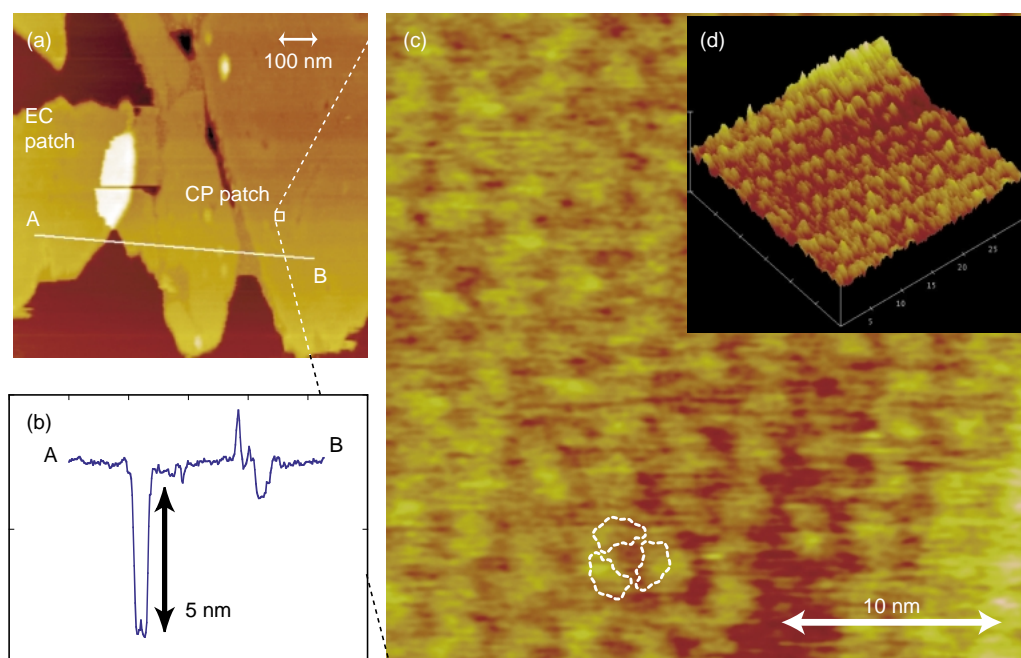


Fig. 4. (a) Topographic AFM image of purple membrane on mica surface. (b) Cross-sectional image along the line indicated in (a). (c) Trimers of bR on cytoplasmic patch can be clearly distinguished. (d) 3D reconstructed image of (c). (EC: extracellular, CP: cytoplasmic)

(<1 nN) acting between the probe and the sample is detected and a topographic image is obtained [19]. The “tapping mode” AFM operation drastically shortens the interaction time between the probe and sample, so it substantially reduces frictional forces and damage to the sample during imaging [20]. This method is particularly effective for imaging soft materials such as proteins, DNA, and other biological molecules. The morphology of purple membrane surfaces and the mechanical properties of bR have previously been measured with high resolution in aqueous conditions [14]. Physical manipulation of the protein using the tip of an AFM probe has also been reported [15], [16].

First, we performed AFM imaging of purple membrane on mica, which is the established substrate for AFM of biomaterials [14], [15], [17]. Purple membranes of *Halobacterium salinarium* strain S9 (>99% pure) were obtained from Sigma-Aldrich Corp. (USA). A lyophilized powder<sup>\*7</sup> of the purple membrane was diluted in buffer solution (100 mM KCl, 10 mM tris-HCl, pH 8.0) to the final concentration of 5–50  $\mu\text{g}/\text{ml}$  and adsorbed onto a freshly cleaved mica plate. After incubation for 20 to 30 minutes, 0.2 ml of buffer solution was added and imaging was per-

formed in liquid at room temperature. Membrane patches about 5 nm thick and from 0.5  $\mu\text{m}$  to several micrometers wide were observed, as shown in **Figs. 4(a)** and **(b)**. Judging from the surface morphology (Fig. 4(a)), two types of patch were present: one with a smooth surface and the other with a relatively rough surface. On the basis of previous work by one of the authors (J.F.R) and his coworkers [17], we considered the former to be the extracellular side and the patch with the relatively rough surface to be the cytoplasmic side. For molecular-level studies of mechanical or electrostatic properties, it is important to know which side is present on the device.

**Figures 4(c)** and **(d)** show high-resolution images of the cytoplasmic patch obtained by very soft tapping following the conditions used in ref. [17]. A hexagonal network originating from the 2D crystal of bR can be seen. High-resolution imaging and Fourier analysis enabled us to resolve the trimer shape of bR, with a size of about 2 nm. The results indicate that molecular-scale imaging in physiological conditions is readily obtained and that we can locate the protein structures precisely.

## 2.2 AFM images of purple membranes on the silicon hole pattern

The test device structure we chose to evaluate consisted of an array of electrochemical cells, each 1

\*7 Lyophilized powder: Freeze-dried powder of biological substances

attoliter in volume, fabricated in silicon by a photolithographic technique using synchrotron orbital radiation and dry etching. Each cell was  $100\text{ nm} \times 100\text{ nm}$  square and  $100\text{ nm}$  deep, and the pitch of the pattern was  $500\text{ nm}$ . Electrodes were not connected to the sample device, but the nano-bio device was in the geometry shown in Fig. 3. A hydrophobic surface, which is essential for strong membrane adhesion, was obtained by HF treatment to produce hydrogen-terminated silicon. This surface was imaged with the tapping-mode AFM in air, as shown in Figs. 5(a) and (b). The cross-sectional profile along the line indicated in Fig. 5(b) was analyzed to confirm the shape of the cell (Fig. 5(c)). The measured cell shape was within expectations given the convolution of the cell and AFM tip.

Purple membrane was deposited on the silicon surface in the same manner as for mica and imaged with the tapping-mode AFM in liquid, as shown in Fig. 5(d). Some of the cells were covered by patches of the membrane, which extended from about  $500\text{ nm}$  to several micrometers in width. A high-magnification

image of the suspended membrane over the cell is shown in Fig. 5(e). The cross sectional line-profile between A and B, shown in Fig. 5(f), clearly shows that the membrane sagged slightly over the cell, as shown by the blue arrow, while a relatively deep hole remained in the area where the membrane incompletely covered the cell (indicated by the red arrow). The depression, which was estimated to be  $5\text{--}10\text{ nm}$  deep, could be due to the interaction between the AFM probe and the membrane during tapping-mode imaging. However, rupture of the membrane by the AFM probe was never observed. Protein suspended over the cell was free from interactions with the substrate, so it should retain its original configuration and function. This structure could therefore provide an ideal electrical platform for observing a functioning membrane protein [2].

### 2.3 Effects of modified silicon surface on the deposition of purple membrane

In the next stage of the fabrication of the proposed device (shown in Fig. 3), the cells filled with buffer

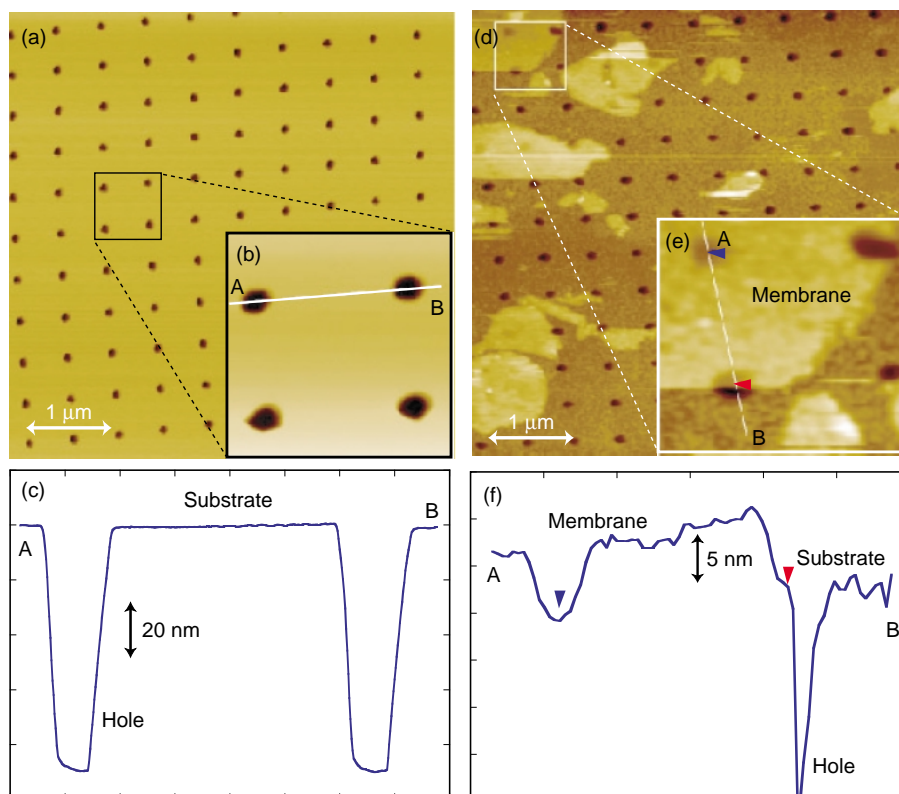


Fig. 5. Topographic AFM image ( $5 \times 5\ \mu\text{m}^2$ ) of the cell pattern on H-terminated silicon measured in air (a) and purple membrane on the pattern surface measured in buffer solution ( $100\text{ mM KCl}$ ) (d). Here, (b) and (e) are magnified images ( $800 \times 800\ \text{nm}^2$ ) of (a) and (d), respectively, and (c) and (f) are cross-sectional images along the lines indicated in (b) and (e), respectively.

solution should be isolated from the outside by forming a highly resistive seal between the bio-membrane and silicon surface [21]. From the viewpoint of semiconductor device processing, insulators such as silicon dioxide and silicon nitride are the preferred materials for the top-most surface to electrically separate the electrodes in different cells and separate them from the counter electrodes. They form flat, stable surfaces and their manufacturing processes are well established. For these reasons we evaluated both silicon dioxide and silicon nitride in the present device configuration.

AFM topographic images of silicon nitride, silicon dioxide, and hydrogen-terminated silicon substrates are shown in **Figs. 6(a), (b), and (c)**, respectively. The insets show magnified images and their line-profiles (**Figs. 6(d), (e), and (f)**) and indicate that their surfaces provide a flat profile for the attachment of bio-membranes. The measured root-mean-square roughnesses were 0.42, 0.41, and 0.15 nm, respectively. To determine the degree of hydrophilicity/hydrophobic-

ity, the contact angles were measured to be  $17.8^\circ$ ,  $28.6^\circ$ , and  $73.8^\circ$ , respectively. Hydrophilicity/hydrophobicity may be one of the important factors determining the strength of the interaction between membrane and substrate. As expected, silicon nitride and silicon dioxide surfaces were hydrophilic.

Purple membrane was deposited on each substrate, in the same manner as described before and imaged in liquid with 0 to 500 mM of salt, as shown in **Figs. 6(g)–(l)**. The interaction between the membrane and substrate was influenced by the salt concentration of the buffer solution. On hydrogen-terminated silicon, the attachment of purple membrane was good, and there was little difference between 250 mM (**Fig. 6(i)**) and 500 mM (**Fig. 6(l)**). In contrast, on silicon nitride and silicon dioxide, the attachment of purple membrane was not good enough. In the case of 250 mM KCl, as shown in **Figs. 6(g) and (h)**, only a few patches of purple membrane attached. The straight edge of the membrane (blue arrows) along the scanning direction indicates that the deposited membrane

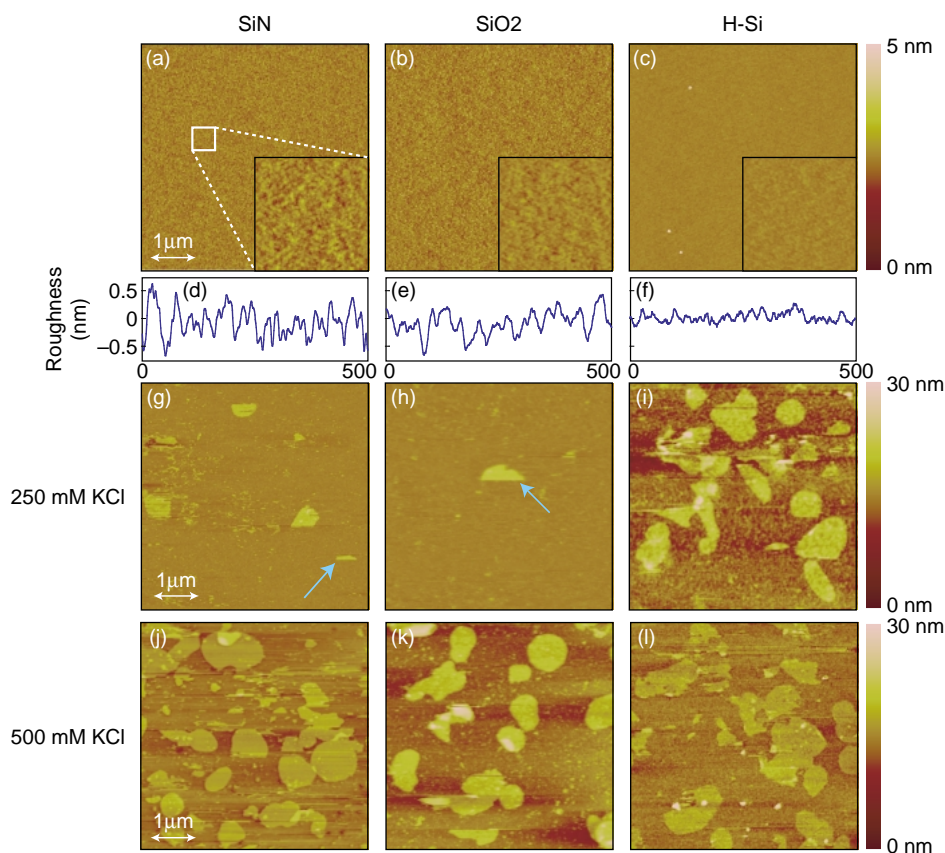


**Fig. 6.** Topographic AFM images ( $5 \times 5 \mu\text{m}^2$ ) of silicon nitride surface (a), silicon dioxide surface (b), and hydrogen-terminated silicon surface (c) before deposition of purple membrane measured in air. Insets show magnified images ( $500 \times 500 \text{nm}^2$ ). (d)–(f) Cross-sections of the magnified images. (g)–(l) Topographic AFM images ( $5 \times 5 \mu\text{m}^2$ ) of purple membrane deposited on each surface.

peeled off during AFM imaging. In subsequent scans of the same area, no membrane was visible, probably because it peeled off. We found that a salt concentration higher than 500 mM was required (Figs. 6(j) and (k)). Therefore, this preliminary study showed that it will be important to optimize the salt concentration and the surface properties in order to provide a good seal between the bio-membrane and the lip of the fabricated cell.

### 3. Summary

We described a way of using biological materials to develop a new type of electronic device. Using AFM, we observed the periodical hexagonal shape of bR on mica. We succeeded in imaging a membrane protein suspended over artificially fabricated cells prepared on a silicon substrate with submicrometer dimensions. Molecular-scale imaging was readily obtained and the structure of the protein being used for the device could be located precisely. The results show that an electrical platform with a functioning membrane protein was provided. We also found that surface modification and the salt concentration of the buffer solution affected the attachment of the membrane protein to form a highly resistive seal with the fabricated cell.

Before we can make a new device using functional biomolecules, we need to improve the fabrication techniques and understand the mechanisms of proteins. We must also learn how to place proteins in specific locations accurately. In the final stage of device fabrication, electrodes will be incorporated into the individual cells to permit discrete electrical measurements. The functional modification of proteins is also something that we will pursue. Imaging with molecular-scale resolution will help clarify the mechanism governing the appearance of biomolecular functions. Molecular-level studies on mechanical and electrical/electronic analysis are also in progress. We also hope to elucidate the conformational change by real-time imaging, leading to an investigation of the dynamics of proteins function. The results will contribute to the integration of biomolecular functions into new devices.

### Acknowledgments

We thank Kislun Voitchovsky (Univ. of Oxford), Sonia A. Contera (Univ. of Oxford), and Kazuaki Furukawa (NTT BRL) for fruitful discussions, suggestions, and assistance. We also thank Masahiro

Uchibatake (NTT-AT) and Miho Kanazawa (NTT-AT) for their excellent technical assistance. This work was conducted as part of the joint bio-nanoscience collaboration between NTT Basic Research Laboratories and the University of Oxford.

### References

- [1] R. R. Birge, N. B. Gillespie, E. W. Izaguirre, A. Kusnetzow, A. F. Lawrence, D. Singh, Q. W. Song, E. Schmidt, J. A. Stuart, S. Seetharaman, and K. J. Wise, "Biomolecular Electronics: Protein-Based Associative Processors and Volumetric Memories," *J. Phys. Chem. B*, Vol. 103, pp. 10746-10766, 1999.
- [2] W. Römer, Y. H. Lam, D. Fisher, A. Watts, W. B. Fischer, P. Göring, R. B. Wehrspohn, U. Gösele, and C. Steinem, "Channel Activity of a Viral Transmembrane Peptide in Micro-BLMs: Vpu<sub>1-32</sub> from HIV-1," *J. American Chem. Soc.* Vol. 126, pp. 16267-16274, 2004.
- [3] D. Oesterhelt and W. Stoekenius, "Isolation of the cell membrane of *Halobacterium halobium* and its fractionalization into red and purple membrane," *Meth. Enzymol.*, Vol. 31, pp. 667-678, 1974.
- [4] D. Oesterhelt and W. Stoekenius, "Function of a new photoreceptor membrane," *Proc. Natl. Acad. Sci. USA*, Vol. 70, pp. 2853-2857, 1973.
- [5] W. Stoekenius, "Bacterial rhodopsin: evolution of a mechanistic model for the ion pumps," *Protein Sci.*, Vol. 8, pp. 447-459, 1999.
- [6] L.-O. Essen, R. Siegert, W. D. Lehmann, and D. Oesterhelt, "Lipid patches in membrane protein oligomers: Crystal structure of the bacteriorhodopsin-lipid complex," *Proc. Natl. Acad. Sci. USA*, Vol. 95, pp. 11673-11678, 1998.
- [7] A. E. Blaurock and W. Stoekenius, "Structure of the purple membrane," *Nature New Biol.*, Vol. 233, pp. 152-154, 1973.
- [8] R. Henderson, J. M. Baldwin, T. A. Ceska, F. Beckman, and K. H. Downing, "Model for the structure of bacteriorhodopsin based on high-resolution electron cryo-microscopy," *J. Mol. Biol.*, Vol. 213, pp. 899-929, 1990.
- [9] Y. Kimura, D. G. Vassilyev, A. Miyazawa, A. Kidera, M. Matsushima, K. Mitsuoka, K. Murata, T. Hirai, and Y. Fujiyoshi, "Surface of bacteriorhodopsin revealed by high-resolution electron crystallography," *Nature*, Vol. 389, pp. 206-211, 1997.
- [10] J. S. Jubb, D. L. Worcester, H. L. Crespi, and G. Zaccari, "Retinal location in purple membrane of *Halobacterium halobium*: a neutron diffraction study of membranes labeled *in vivo* with deuterated retinal," *EMBO J.*, Vol. 3, pp. 1455-1461, 1984.
- [11] N. Hampp, "Bacteriorhodopsin as a photochromic retinal protein for optical memories," *Chem. Rev.*, Vol. 100, pp. 1755-1776, 2000.
- [12] H. Trissl, "Photoelectric measurements of purple membranes," *Photochem. Photobiol.*, Vol. 51, pp. 793-818, 1990.
- [13] H. Choi, J. Min, K. K. Han, J. W. Choi, and W. H. Lee, "Photoelectric conversion of bacteriorhodopsin films fabricated by self-assembly technique," *Synth. Met.*, Vol. 117, pp. 141-143, 2001.
- [14] D. J. Müller, F. A. Schabert, G. Büldt, and A. Engel, "Imaging purple membranes in aqueous solutions at subnanometer resolution by atomic force microscopy," *Biophys. J.*, Vol. 68, pp. 1681-1686, 1995.
- [15] D. J. Müller, G. Büldt, and A. Engel, "Force-induced conformational change of bacteriorhodopsin," *J. Mol. Biol. J.*, Vol. 249, pp. 239-243, 1995.
- [16] F. Oesterhelt, D. Oesterhelt, M. Pfeiffer, A. Engel, H. E. Gaub, and D. J. Müller, "Unfolding pathways of individual bacteriorhodopsins," *Science*, Vol. 288, pp. 143-146, 2000.
- [17] K. Voitchovsky, S. A. Contera, M. Kamihira, A. Watts, and J. F. Ryan, "Differential stiffness and lipid mobility in the leaflets of purple membranes," *Biophys. J.*, Vol. 90, pp. 2075-2085, 2006.
- [18] V. J. Morris, A. R. Kirby, and A. P. Gunning, "Atomic force microscopy for biologists," Imperial College Press, 1999.
- [19] G. Binning, C. F. Quate, and Ch. Gerber, "Atomic force microscope," *Phys. Rev. Lett.* 56, pp. 930-933, 1986.

- [20] P. K. Hansma, J. P. Cleveland, M. Radmacher, D. A. Walters, P. E. Hillner, M. Bezanilla, M. Fritz, D. Vie, H. G. Hansma, C. B. Prater, J. Massie, L. Fukunaga, J. Gurley, and V. Elings, "Tapping mode atomic force microscopy in liquids," *Appl. Phys. Lett.* 64, pp. 1738-1740, 1994.

- [21] Md. M. Rahman, Y. Nonogaki, R. Tero, Y-H. Kim, H. Uno, Z-L. Zhang, T. Yano, M. Aoyama, R. Sasaki, H. Nagai, M. Yoshida, and T. Uris, "Giant vesicle fusion on microelectrodes fabricated by femtosecond laser ablation followed by synchrotron radiation etching," *Jpn. J. Appl. Phys.* Vol. 44, pp. L1207-L1210, 2005.



#### **Koji Sumitomo**

Senior Research Scientist, NTT Basic Research Laboratories.

He received the B.E., M.E., and Ph.D. degrees in electronics from Osaka University, Osaka, in 1986, 1988, and 1991, respectively. He joined NTT Basic Research Laboratories in 1991. Since then, he has been engaged in research on the characterization and control of nanostructures on semiconductor surfaces. His current work includes research on nano-bio technologies. He is a member of the Physical Society of Japan, the Japan Society of Applied Physics (JSAP), the Surface Science Society of Japan, the American Vacuum Society, and the Materials Research Society.



#### **Keiichi Torimitsu**

Executive Manager, Materials Science Laboratory, Group Leader, Molecular and Bio Science Research Group, NTT Basic Research Laboratories.

He received the B.E., M.E., and Ph.D. degrees in instrumentation engineering from Keio University, Kanagawa, in 1980, 1982, and 1986, respectively. In 1986, he joined NTT Basic Research Laboratories and worked in the bio-computer project. He is currently focusing on nano-bio science and nano-bio device fabrication. He is a member of the Society for Neuroscience, International Brain Research Organization, Japan Neuroscience Society, JSAP, and the Japanese Pharmacological Society.



#### **Hiroshi Nakashima**

Research Scientist, NTT Basic Research Laboratories.

He received the B.E., M.E., and Ph.D. degrees in applied chemistry from Waseda University, Tokyo, in 1995, 1997, and 2002, respectively. He joined NTT Basic Research Laboratories in 1997. Since then, he has been engaged in research on the synthesis and control of optoelectrical properties of (semi)conductive polymers. His current work includes research on nano-bio technologies. He is a member of the Chemical Society of Japan, the Society of Polymer Science, Japan, and the Society of Silicon Chemistry, Japan.



#### **Chandra Ramanujan**

NTT Bionanoscience Research Fellow, Department of Physics, University of Oxford.

He received the Ph.D. degree in atomic force microscopy and nanomechanics from the University of Oxford and is currently a member of the joint bionanoscience collaboration between NTT Basic Research Laboratories and Oxford University.



#### **Mime Kobayashi**

Research Associate, NTT Basic Research Laboratories.

He received the B.S. degree in agricultural chemistry from Kyoto University, Kyoto, and the M.S. and Ph.D. degrees in biological sciences from Nara Institute of Science and Technology, Nara, in 1994, 1996, and 1999, respectively. He was a post-doctoral associate in the department of Pharmacology at Weill Medical College of Cornell University before joining NTT Basic Research Laboratories in 2004. His current work includes research on nano-bio technologies. He is a member of the Biophysical Society (USA) and the Molecular Biology Society of Japan.



#### **John F. Ryan**

Professor of Physics and Director of the Bionanotechnology Interdisciplinary Research Collaboration, University of Oxford.

He is a graduate of Edinburgh University. His research has focused on quantum optoelectronics and semiconductor nanostructures, and his current interests include bionanostructures and devices, membrane proteins, and scanning probe microscopy.